Pure Appl. Chem., Vol. 85, No. 7, pp. 1405–1413, 2013.
http://dx.doi.org/10.1351/PAC-CON-12-08-05

Light-driven hydrogen evolution system with glutamic-acid-modified zinc porphyrin as photosensitizer and [FeFe]-hydrogenase model as catalyst*

Shan Yu, Feng Wang, Jing-Jing Wang, Hong-Yan Wang, Bin Chen, Ke Feng, Chen-Ho Tung, and Li-Zhu Wu‡

Key Laboratory of Photochemical Conversion and Optoelectronic Materials, Technical Institute of Physics and Chemistry, the Chinese Academy of Sciences, Beijing 100190, China

Abstract: An intermolecular light-driven hydrogen evolution system with free glutamic-acid-modified zinc tetra(*p*-phenyl) porphyrin (**Glu-ZnP**) as a photosensitizer and $[Fe_2(CO)_6(\mu\text{-adt})C_6H_5]$ [μ-adt = $N(CH_2S)_2$] (**Badt**) as a catalyst has been constructed. Using phenylmercaptan (**BSH**) as electron donor and acetic acid (HOAc) as proton source, hydrogen was obtained after irradiation with visible light for 2 h; the efficiency is comparable to that of the similar intramolecular dyad. Steady-state and time-resolved spectroscopy and cyclic voltammetry show that both the first and the second electron transfer from singlet ^{1*}**Glu-ZnP** to **Badt** and reduced **Badt** are thermodynamically feasible. However, the competition of electron transfer from singlet ^{1*}**Glu-ZnP** to **Badt** with intersystem crossing from singlet ^{1*}**Glu-ZnP** to triplet ^{3*}**Glu-ZnP**, inefficient electron transfer from triplet ^{3*}**Glu-ZnP** to **Badt**, and the lower energy of triplet ^{3*}**Glu-ZnP** and possible ^{3*}**Badt** to that of yielded charge-separated state of **Glu-ZnP**$^{+\cdot}$**-Badt**$^{-\cdot}$ were believed to be the obstacles for efficient hydrogen evolution.

Keywords: back electron transfer; energy transfer; [FeFe]-hydrogenase; [2Fe2S] model; intersystem crossing; light-driven hydrogen evolution; photoinduced electron transfer; zinc porphyrin.

INTRODUCTION

[FeFe]-hydrogenase, an enzyme existing in certain bacteria and algae, has remarkable catalytic efficiency in proton reduction (6000–9000 molecules hydrogen s^{-1} per site) [1,2]. In the late 1990s, the active site of [FeFe]-hydrogenase was structurally resolved, which contains a cubic [4Fe4S] unit covalently linking to a butterfly-like [2Fe2S] unit through coordination with S atom of cysteine [3,4]. The low-cost elements composition and high catalytic efficiency in proton reduction of the active site have inspired chemists to develop electrocatalytic or photocatalytic hydrogen evolution systems with [2Fe2S] models [5–13]. From a photochemical point of view, a variety of [2Fe2S] models have been employed to construct artificial photosynthetic systems and to understand the mechanism of proton reduction by [2Fe2S] models. These systems, however, were unable to produce hydrogen

Pure Appl. Chem.* **85, 1257–1513 (2013). A collection of invited papers based on presentations at the XXIVth IUPAC Symposium on Photochemistry, Coimbra, Portugal, 15–20 July 2012.
‡Corresponding author

photochemically until 2008. Sun and co-workers reported the first photochemical example for hydrogen evolution using ruthenium complex as a photosensitizer, [2Fe2S] model as a catalyst, and phenylmercaptan (**BSH**) as a sacrificial electron donor, in a mixture of acetonitrile and water [13]. Since then, great progress has been made in this field. The turnover number (TON) of the artificial [2Fe2S] model systems has been increased from null to more than 500 under visible light and 2600 under UV light [14,15]. Our investigations to achieve light-driven hydrogen evolution by [2Fe2S] models, including molecular dyads and a triad, a self-assembling biomimetic system, and quantum dots/[2Fe2S] model hybrid system, have been reported in a series of papers [14,16–20]. Of these systems, noble metal (Ru^{II}, Ir^{III}, Re^{I}, Pt^{II}) complexes, organic dyes, and even quantum dots have been used as photosensitizers for hydrogen evolution [13–22].

Porphyrins derivatives, which exist in chlorophyll pigments in nature and could absorb as much as 46 % of sunlight, should be ideal photosensitizers in light-driven hydrogen production systems. Combining the natural building-blocks [2Fe2S] unit as proton reduction catalytic center and porphyrin derivatives as photosensitizer, scientists have constructed several molecular dyads or triads [23–28]. Song et al. described a dyad, in which a zinc porphyrin moiety and a pyridine-functionalized [2Fe2S] unit were locked by coordination, but no hydrogen was detected when the system was illuminated with visible light [23]. Later, Reek et al. constructed a butterfly-like supramolecule with two different zinc porphyrins and one [2Fe2S] unit [25]. By illumination with visible light, this assembly could produce hydrogen with TON of 2. But the detailed mechanism for photoinduced hydrogen production was unclear. Very recently, Wasielewski et al. demonstrated photoinduced electron transfer from zinc porphyrin to [2Fe2S] unit in both covalently linked dyads and triads [26,27]. Nevertheless, the efficiency for photochemical hydrogen evolution from porphyrin derivatives and [2Fe2S] models is lower than that of the other reported systems [23–28].

In 2008, Sun and Pan reported a self-assembling dyad containing one zinc tetraphenyl-porphyrin and one [2Fe2S] unit with a pyridyl group [28]. In the presence of 2-mercaptobenzoic acid and trifluoroacetic acid, this dyad enables hydrogen production under visible light irradiation, but *no* hydrogen could be detected from the corresponding intermolecular system. Particular interest in light-driven hydrogen evolution from [2Fe2S] model [14,16–20] prompted us to study the intermolecular system with free glutamic-acid-modified zinc tetra(*p*-phenyl) porphyrin (**Glu-ZnP**) as photosensitizer and $[Fe_2(CO)_6(\mu\text{-adt})C_6H_5]$ [μ-adt = $N(CH_2S)_2$] (**Badt**) as catalyst (Scheme 1). To avoid the possible

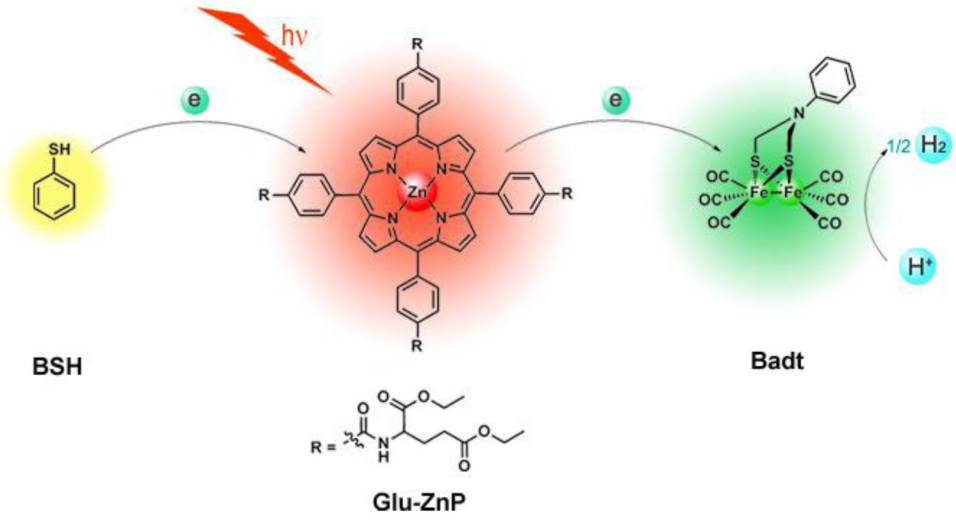

Scheme 1 The intermolecular system for light-driven hydrogen evolution.

coordination between zinc atom in **Glu-ZnP** and nitrogen atom in **Badt** and hence the formation of supramolecular system, glutamic acid diethyl ester was introduced into the porphyrin backbone, and steric group benzyl on **Badt** can also decrease the possibility of coordination between **Glu-ZnP** and **Badt**. The molecular design is to ensure the free state of photosensitizer and catalyst in solution. With visible light irradiation, this system is able to produce hydrogen in the presence of **BSH** as electron donor and acetic acid (HOAc) as proton source, and TON of 0.87 is achieved after irradiation of 2 h; the efficiency of which is comparable to that of the intramolecular dyad [28]. Furthermore, the steady-state and time-resolved spectroscopy and cyclic voltammetry were used to understand the intermolecular photoinduced electron-transfer processes necessary for hydrogen evolution. The results have shown that the first and the second electron transfer from singlet ^{1*}**Glu-ZnP** to **Badt** and reduced **Badt** are both thermodynamically feasible, while intersystem crossing, energy transfer, and back electron transfer processes might lead to the low efficiency of the light-driven hydrogen evolution system.

MATERIALS AND METHODS

CH_3OH (Fisher Chemicals, HPLC grade), CH_3CN (Fisher Chemicals, HPLC grade), phenyl-mercaptan (Alfa Aesar), tetra(*p*-carboxyphenyl) porphyrin (Sigma-Aldrich). Deionized water was employed to prepare the sample for photocatalytic reactions. CH_2Cl_2 (Fisher Chemicals, HPLC grade) for reactions was distilled under argon atmosphere from CaH_2 before use. Tetrahydrofuran (THF, Fisher Chemicals, HPLC grade) for reactions was distilled under argon atmosphere from metal Na before use.

^{1}H NMR spectra were run on a Bruker-400 spectrometer with tetramethylsilane (1H) as internal standard. Matrix-assisted laser desorption/ionization with time-of-flight (MALDI-TOF) mass spectrometry was performed on a BIFLEXIII MALDI-TOF mass spectrometer. High-resolution electrospray ionization mass spectroscopy (HR-ESI-MS) was performed on a Bruker APEX III 7.0 Tesla FTICR Mass spectrometer combined with Apollo ESI source. Elemental analyses were determined on a FLASH EA1112 elemental analyzer. UV–vis absorption spectra were recorded using a Shimadzu 1601 PC spectrophotometer. Emission spectra were determined on a Hitachi 4500 spectrophotometer. Time-resolved emission and transient absorption spectroscopy were carried out on Edinburgh LP 920. The hydrogen production experiment was performed in a Pyrex tube by irradiation with a 500 W high-pressure Hanovia mercury lamp. A glass filter (Edmund Optics GG-400) was used to cut off light below 400 nm to guarantee the irradiation of visible light. Hydrogen detection was carried out on a Shimadzu GC-14B instrument with methane as an internal standard. The response factor for hydrogen to methane determined by calibration with known amounts of hydrogen and methane was 3.0 under the experimental conditions. Electrochemical investigation was studied on a Princeton Applied Research Potentionstat-gravanostat model 283. A three-electrode system containing a 3-mm glassy carbon working electrode, a platinum wire counter electrode, and a nonaqueous Ag/Ag^+ reference electrode was used to conduct the cyclic voltammetric experiments. Before measurement, the glassy carbon electrode was polished with a 0.05 μm alumina paste and sonicated for 15 min, and the electrolyte solution (0.1 M *n*-Bu_4NPF_6) was deoxgenated with argon for 30 min.

EXPERIMENTAL

Synthesis of Glu-ZnP

Tetra(*p*-carboxyphenyl) porphyrin (0.40 g, 0.5 mmol) was suspended in a three-necked round-bottom flask with freshly distilled CH_2Cl_2. The flask was then flushed with nitrogen. Excess L-glutamic acid diethyl ester hydrochloride (0.72 g, 3.0 mmol) was added, followed by the addition of *N*,*N*,*N*′,*N*′-tetramethyl-*O*-(benzotriazol-1-yl)uronium tetrafluoroborate (TBTU, 0.64 g, 2.0 mmol), 1-hydroxy-

benzotrizole (HOBt, 0.12 g, 0.8 mmol), *N*,*N*-diisopropylethylamine (DIEA, 0.40 g, 3.2 mmol), and pyridine (0.5 mL). The mixture was then stirred at room temperature overnight. Upon removal of the solvent in vacuum, the residue was purified by silica gel column chromatography with CH_2Cl_2/THF as the eluent to yield the precursor of **Glu-ZnP**. Then, the precursor of **Glu-ZnP** (153 mg, 0.10 mmol) and $Zn(OAc)_2$ (18 mg, 0.10 mmol) were dissolved in a mixed solvent of CH_2Cl_2 and CH_3OH. The mixture was then stirred at 40 °C for 3 h. After removal of the solvent, the crude product was subjected to silica gel column chromatography with CH_2Cl_2/CH_3OH as the eluent to give the deep purple product in a yield of 32 %. ^{1}H NMR (400 MHz, $CDCl_3$, ppm): δ = 1.23 (t, J = 7.0 Hz, 12H), 1.35 (t, J = 7.0 Hz, 12H), 2.09 (m, 4H), 2.27 (m, 4H), 2.45 (m, 8H), 4.07 (q, J = 7.2 Hz, 8H), 4.27 (q, J = 7.2 Hz, 8H), 4.66 (m, 4H), 7.22 (d, J = 7.2 Hz, 4H), 7.97 (d, J = 8.0 Hz, 8H), 8.27 (d, J = 8.0 Hz, 8H), 8.89 (s, 8H). ^{13}C NMR ($CDCl_3$, 100 MHz, ppm): δ = 173.4, 171.9, 167.0, 149.9, 146.6, 134.7, 132.4, 132.0, 125.2, 120.1, 61.9, 60.9, 52.4, 30.5, 27.1, 14.3, 14.2. Anal. Calcd. for $C_{84}H_{88}N_8O_{20}Zn\cdot(CH_2Cl_2)_{0.5}$: C, 61.98; H, 5.48; N, 6.84. Found: C, 61.77; H, 5.48; N, 6.90. MALDI-TOF MS: m/z = 1595 $[M + H]^+$.

Synthesis of Badt

Aniline (0.46 g, 4.9 mmol) and paraformaldehyde (0.38 g) in 10 mL CH_2Cl_2 were stirred for 2 h at room temperature under an argon atmosphere. Then $SOCl_2$ (0.88 mL, 4.4 mmol) was added dropwise. After further reaction of 1 h, the system was dried by the argon flow and the residue was then added into the THF solution of $Li_2[Fe_2S_2(CO)_6]$ [30] (0.72 g, 2.0 mmol) to allow another reaction for 3 h at room temperature. Finally, the solvent was moved away and the residue was subjected to silica gel column chromatography with petroleum ether as the eluent. The pure product has a deep red color with a yield of 70 %. ^{1}H NMR (400 MHz, CD_3COCD_3, ppm): δ = 7.31 (m, 2H), 6.94 (d, J = 8.3 Hz, 2H), 6.87 (m, 1H), 4.59 (s, 4H). ^{13}C NMR ($CDCl_3$, 100 MHz, ppm): δ = 207.0, 144.7, 129.9, 120.4, 115.9, 49.8. Anal. Calcd. for $C_{14}H_9Fe_2NO_6S_2$: C, 36.33; H, 1.96; N, 3.03. Found: C, 36.27; H, 1.98; N, 3.11. HR-ESI-MS: m/z = 485.23 $[M + Na]^+$.

RESULTS AND DISCUSSION

Glu-ZnP was synthesized according to the literature [29] except that the coupling reagents were replaced by TBTU/HOBt/DIEA. **Badt** was prepared based on the procedure in the literature [30]. Both compounds were characterized by ^{1}H NMR, ^{13}C NMR, MS, and elementary analysis. Because no band shift in the UV–vis absorption spectra of **Glu-ZnP** in CH_3CN was observed during titration experiments with **Badt** (Fig. 1), we think there is no strong intermolecular interaction between **Glu-ZnP** and **Badt** in the ground state.

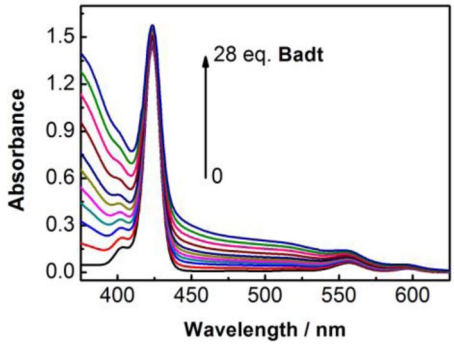

Fig. 1 UV–vis absorption spectra of **Glu-ZnP** (5.0×10^{-6} M in CH_3CN) in the absence and presence of **Badt** with different equivalents.

Electrochemical study can provide redox potential of compounds and thus some detailed information on proton reduction process of the system. Here, we utilized cyclic voltammetry to investigate the electrochemical behavior of **Badt** in CH_3CN. As shown in Fig. 2a, the first quasi-reversible reduction peak at –1.53 V (E^1_{pc}) (all potentials reported here vs. Fc/Fc^+) is attributed to the one-electron reduction of Fe(I)Fe(I) to Fe(I)Fe(0) of **Badt**, and the oxidation potential at 0.62 V is ascribed to the oxidation of Fe(I)Fe(I) to Fe(I)Fe(II) of **Badt**. With the addition of 2 equiv of HOAc to the solution of **Badt** (Fig. 2b), the current intensity of the first reduction peak increased slightly. With increasing the concentration of HOAc, the second reduction peak corresponding to Fe(I)Fe(0) to Fe(0)Fe(0) of **Badt** emerged at –1.72 V (E^2_{pc}). The current intensity of both reduction peaks is proportional to the concentration of HOAc in solution. Since electrolysis of HOAc without catalyst occurs at more negative potential (–1.96 V) [31,32], this reduction event is attributed to the electrochemical catalytic proton reduction process, in which **Badt** functions as catalyst [10,12,33]. The response of current density at E^2_{pc} vs. the concentration of HOAc is more sensitive than that at E^1_{pc}, which means that the catalytic proton reduction that occurred at E^2_{pc} was more efficient when weak acid HOAc was used as the proton source in electrocatalytic system.

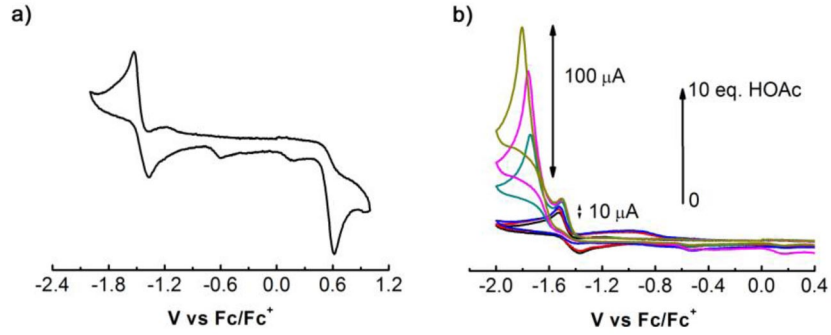

Fig. 2 Cyclic voltammograms of **Badt** (a) and its electrochemical response with the addition of HOAc (0–10 equiv) (b) with 1.0 mM in 0.1 M n-Bu_4NPF_6/CH_3CN. Scan rate: 100 mV/s; working electrode: glassy carbon electrode; reference electrode: Ag/Ag^+ electrode. All potentials vs. Fc/Fc^+.

The photochemical reaction for hydrogen evolution using **Glu-ZnP** as the photosensitizer and **Badt** as the catalyst was carried out in a mixed solution of CH_3CN/H_2O (V/V = 1/1) at room temperature, where **BSH** and HOAc function as sacrificial electron donor and proton source, respectively. As shown in Fig. 3, the amount of hydrogen evolved from the system increased immediately in the first

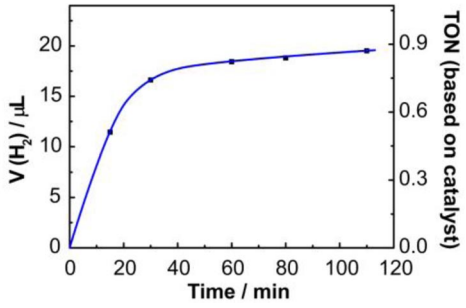

Fig. 3 Time dependence of hydrogen evolution in CH_3CN/H_2O (V/V = 1/1). [**Glu-ZnP**] = 1.0×10^{-4} M, [**Badt**] = 1.0×10^{-4} M, [**BSH**] = 0.05 M and [HOAc] = 0.1 M.

30 min. Further irradiation of the system made no obvious improvement of hydrogen production accompanying with the formation of precipitates, similar to other reported [2Fe2S] models [13,28]. Control experiments have shown that no hydrogen formation was observed when any component of light, **Glu-ZnP**, **Badt** and **BSH** was omitted. The amount of hydrogen has reached a plateau of 19.5 μL with TON of 0.87 (based on either **Glu-ZnP** or **Badt**).

To better understand the interaction between **Glu-ZnP** and **Badt**, we examined fluorescence spectra of **Glu-ZnP** in the absence and presence of **Badt** in CH_3CN. As shown in Fig. 4, **Glu-ZnP** shows two intense fluorescence bands at about 602 and 652 nm after excited at 420 nm, analogous to most of the porphyrin derivatives [34,35]. With the addition of **Badt** into the solution, the fluorescence of **Glu-ZnP** was quenched obviously, suggesting the strong interaction between **Glu-ZnP** and **Badt** in the excited state. Because there is little overlap between the absorption spectrum of **Badt** and the fluorescence spectrum of **Glu-ZnP**, the energy transfer from singlet ^{1*}**Glu-ZnP** to **Badt** can be excluded. So the fluorescence quenching of **Glu-ZnP** was tentatively attributed to the electron transfer from singlet ^{1*}**Glu-ZnP** to **Badt**. The quenching process obeys the Stern–Volmer equation (Fig. 4, inset) with a quenching constant k_S of 1.89×10^{12} $M^{-1}{\cdot}s^{-1}$.

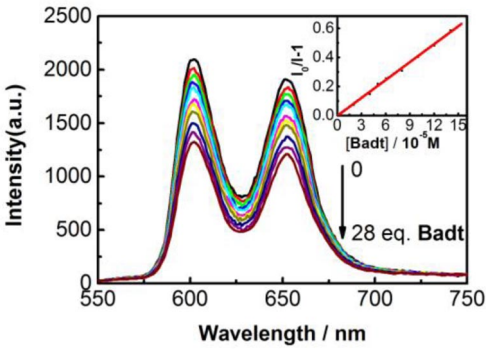

Fig. 4 Fluorescence spectra of **Glu-ZnP** in CH_3CN (2.0×10^{-5} M) in the absence and presence of **Badt** (0 to 1.4×10^{-4} M); excitation wavelength: 420 nm. Inset: Stern–Volmer curve of **Glu-ZnP** with the concentration of **Badt**.

Transient absorption measurements were also utilized to address the possible electron-transfer process in the system. Due to the fast intersystem crossing from singlet to triplet state of **Glu-ZnP** [34,36], the absorption spectra characteristic of the singlet ^{1*}**Glu-ZnP** could not be detected by the equipment with nanosecond resolution. Instead, a strong absorption at 455 nm and a broad absorption from 610 to 800 nm appeared, along with the bleach of the ground state absorption of **Glu-ZnP** at about 560 and 600 nm (Fig. 5a), all of which are typical triplet ^{3*}**Glu-ZnP** [34]. According to kinetic traces at 470 nm, the lifetime of triplet ^{3*}**Glu-ZnP** was calculated to be 78.9 μs. As **Badt** was added into the solution, no signals characteristic of Fe(I)Fe(0) state [11] could be detected. The shape of the whole transient absorption spectra of **Glu-ZnP** was almost the same (Fig. 5b), but the lifetime of triplet ^{3*}**Glu-ZnP** at 470 nm was shortened to 2.5 μs, which is consistent with that of similar triplet species reported by Wasielewski et al. [26]. The decay might originate from the energy transfer from triplet ^{3*}**Glu-ZnP** to possible ^{3*}**Badt**. According to Stern–Volmer equation, the quenching constant (k_T) was determined to be 1.9×10^9 $M^{-1}{\cdot}s^{-1}$, suggesting the quenching is a diffusion-controlled process.

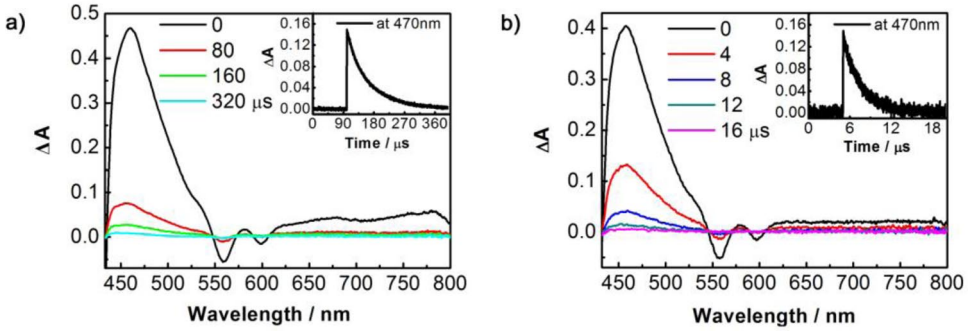

Fig. 5 Transient absorption spectra of **Glu-ZnP** (2.0×10^{-5} M in CH_3CN) in the absence (a) and presence (b) of **Badt** (2.0×10^{-4} M) upon laser pulsed at 423 nm under argon atmosphere; inset: the corresponding kinetic traces recorded at 470 nm.

The spectroscopic and electrochemical analysis studied above allowed us to estimate the free energy changes ($\Delta G°$) of electron-transfer processes that are involved in our system by the Rehm–Weller equation [37]:

$$\Delta G° = E_{ox}(D) - E_{red}(A) - E_{00} - C$$

where E_{00} is the excited-state energy of the photosensitizer; $E_{ox}(D)$ and $E_{red}(A)$ represent the oxidative potential of donor and reductive potential of acceptor, respectively; C is the Coulomb term. In our system, the lowest energy of singlet ^{1*}**Glu-ZnP** (E^{S}_{00}) was determined to be 2.16 eV based on the cross-point (574 nm) of the fluorescence and absorption spectra of **Glu-ZnP**; the lowest energy of triplet ^{3*}**Glu-ZnP** (E^{T}_{00}) was assigned to be 1.53 eV [35]. According to cyclic voltammetry, the oxidative potential of **Glu-ZnP** was at 0.43 eV; the first and the second reductive potential of **Badt** are at –1.53 and –1.72 eV, respectively. As a result of the large dielectric constant of CH_3CN (35.9) [38] used in our system and the relative long distance between donor and acceptor in the intermolecular system, C could be neglected here [39,40]. Taking all these into the Rehm–Weller equation, we found that the first electron transfer from singlet ^{1*}**Glu-ZnP** to **Badt** [Fe(I)Fe(I)] is thermodynamically feasible ($\Delta G^{S}_{ET1} = -0.20$ eV); the second electron transfer from singlet ^{1*}**Glu-ZnP** to the one-electron reduced **Badt** [Fe(I)Fe(0)] is also feasible in spite of rather small free energy change ($\Delta G^{S}_{ET2} = -0.01$ eV). In contrast, the electron transfer from triplet ^{3*}**Glu-ZnP** to **Badt** seems impossible as a result of the blocked uphill ($\Delta G^{T}_{ET1} = +0.43$ eV).

Based on the above experiments and calculations, we speculate the photophysical processes of the intermolecular system as follows (Scheme 2). With illumination of visible light, **Glu-ZnP** is excited to singlet ^{1*}**Glu-ZnP**, which can transfer electron quickly to **Badt**. Following the electron transfer from singlet ^{1*}**Glu-ZnP** to **Badt**, the charge-separated state of **Glu-ZnP**$^{+\cdot}$**-Badt**$^{-\cdot}$ is formed. The generated **Badt**$^{-\cdot}$ [Fe(I)Fe(0)] interacts with proton for hydrogen evolution, while the **Glu-ZnP**$^{+\cdot}$ reacts with sacrificial electron donor **BSH** for regeneration. Afterwards, singlet ^{1*}**Glu-ZnP** can deliver the second electron to the Fe(I)Fe(0) active site of **Badt** upon excitation, but the small driving force makes this photoinduced electron transfer process less effective, thus leading to the relatively small contribution to hydrogen evolution. Singlet ^{1*}**Glu-ZnP** can also transform into triplet ^{3*}**Glu-ZnP** through intersystem crossing. Triplet ^{3*}**Glu-ZnP** is unable to transfer electron to **Badt** because it is a thermodynamically forbidden process. Instead, back electron transfer from charge-separated state of **Glu-ZnP**$^{+\cdot}$**-Badt**$^{-\cdot}$ (including the first and second electron transfer from singlet ^{1*}**Glu-ZnP** to the Fe(I)Fe(I) or Fe(I)Fe(0) active site of **Badt**, respectively) to triplet ^{3*}**Glu-ZnP** is preferred due to the lower energy of the latter. Alternatively, energy transfer from triplet ^{3*}**Glu-ZnP** to possible ^{3*}**Badt** occurs, which may make no contribution to hydrogen evolution.

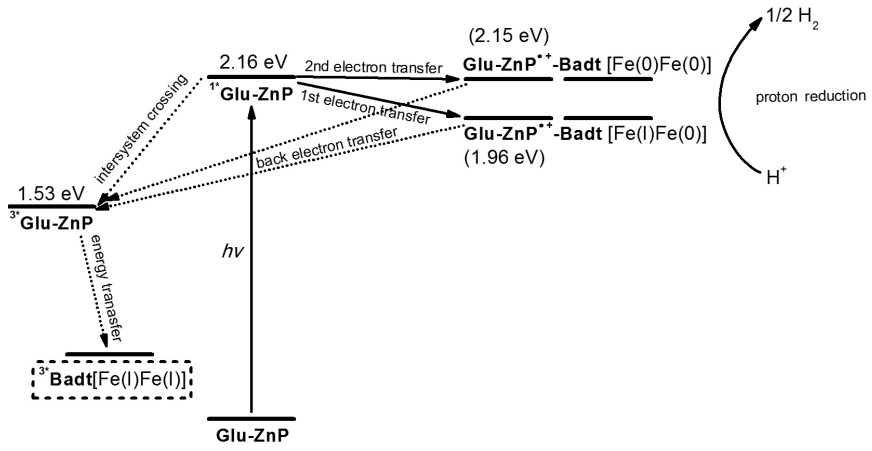

Scheme 2 The energy diagram of the intermolecular system; the solid line arrows correspond to favorable processes, and the dotted line arrows to unfavorable processes for light-driven hydrogen evolution.

CONCLUSION

In summary, an intermolecular light-driven hydrogen evolution system has been constructed, in which **Glu-ZnP** worked as a photosensitizer, **Badt** as a catalyst, **BSH** as an electron donor, and HOAc as a proton source. This system is able to produce hydrogen upon irradiation with visible light. TON of 0.87 was obtained from a mixed CH_3CN/H_2O solution, and this value is comparable to that of the intramolecular dyad. Spectroscopic and electrochemical studies have revealed that electron transfer from singlet ^{1*}**Glu-ZnP** to either **Badt** or one-electron reduced **Badt** was thermodynamically possible. Competition of the electron transfer from singlet ^{1*}**Glu-ZnP** to **Badt** with the intersystem crossing of singlet ^{1*}**Glu-ZnP** to triplet ^{3*}**Glu-ZnP**, ineffective electron transfer from triplet ^{3*}**Glu-ZnP** to **Badt** and lower energy of triplet ^{3*}**Glu-ZnP** to that of charge-separated state of **Glu-ZnP$^{+\cdot}$-Badt$^{-\cdot}$** may be all responsible for the low TON value of this light-driven hydrogen evolution system. We are currently investigating ways to improve the photocatalytic performance via modulating the energy level of both porphyrin derivatives and [2Fe2S] models, and to develop their long-lived charge-separated states for hydrogen evolution in aqueous solutions.

ACKNOWLEDGMENTS

We are grateful for financial support from the Ministry of Science and Technology of China (2009CB22008, 2013CB834505, and 2013CB834804), the National Science Foundation of China (50973125, 21090343, and 91027041), the Solar Energy Initiative of the Knowledge Innovation Program of the Chinese Academy of Sciences, and the Bureau for Basic Research of the Chinese Academy of Sciences.

REFERENCES

1. M. Frey. *ChemBioChem* **3**, 153 (2002).
2. M. L. Ghirardi, A. Dubini, J. Yu, P.-C. Maness. *Chem. Soc. Rev.* **38**, 52 (2009).
3. M. W. W. Adams, E. I. Stiefel. *Science* **282**, 1842 (1998).
4. Y. Nicolet, C. Piras, P. Legrand, C. E. Hatchikian, J. C. Fontecilla-Camps. *Structure* **7**, 13 (1999).
5. C. Tard, C. J. Pickett. *Chem. Rev.* **109**, 2245 (2009).
6. F. Gloaguen, T. B. Rauchfuss. *Chem. Soc. Rev.* **38**, 100 (2009).

7. A. Magnuson, M. Anderlund, O. Johansson, P. Lindblad, R. Lomoth, T. Polivka, S. Ott, K. Stensjö, S. Styring, V. Sundström, L. Hammarström. *Acc. Chem. Res.* **42**, 1899 (2009).
8. M. Wang, L. Sun. *ChemSusChem* **3**, 551 (2010).
9. F. Wang, W.-G. Wang, H.-Y. Wang, G. Si, C.-H. Tung, L.-Z. Wu. *ACS Catal.* **2**, 407 (2012).
10. F. Gloaguen, J. D. Lawrence, T. B. Rauchfuss. *J. Am. Chem. Soc.* **123**, 9476 (2001).
11. S. J. Borg, T. Behrsing, S. P. Best, M. Razavet, X. Liu, C. J. Pickett. *J. Am. Chem. Soc.* **126**, 16988 (2004).
12. R. Mejia-Rodriguez, D. Chong, J. H. Reibenspies, M. P. Soriaga, M. Y. Darensbourg. *J. Am. Chem. Soc*. **126**, 12004 (2004).
13. Y. Na, M. Wang, J. Pan, P. Zhang, B. Åkermark, L. Sun. *Inorg. Chem.* **47**, 2805 (2008).
14. F. Wang, W.-G. Wang, X.-J. Wang, H.-Y. Wang, C.-H. Tung, L.-Z. Wu. *Angew. Chem., Int. Ed.* **50**, 3193 (2011).
15. F. Wen, X. Wang, L. Huang, G. Ma, J. Yang, C. Li. *ChemSusChem* **5**, 849 (2012).
16. W.-G. Wang, F. Wang, H.-Y. Wang, G. Si, C.-H. Tung, L.-Z. Wu. *Chem. Asian J.* **5**, 1796 (2010).
17. H.-Y. Wang, W.-G. Wang, G. Si, F. Wang, C.-H. Tung, L.-Z. Wu. *Langmuir* **26**, 9766 (2010).
18. H.-Y. Wang, G. Si, W.-N. Cao, W.-G. Wang, Z.-J. Li, F. Wang, C.-H. Tung, L.-Z. Wu. *Chem. Commun.* **47**, 8406 (2011).
19. W.-G. Wang, F. Wang, H.-Y. Wang, C.-H. Tung, L.-Z. Wu. *Dalton Trans.* **41**, 2420 (2012).
20. W.-N. Cao, F. Wang, H.-Y. Wang, B. Chen, K. Feng, C.-H. Tung, L.-Z. Wu. *Chem. Commun.* **48**, 8081 (2012).
21. P. Zhang, M. Wang, Y. Na, X. Li, Y. Jiang, L. Sun. *Dalton Trans.* **39**, 1204 (2010).
22. X. Li, M. Wang, L. Chen, X. Wang, J. Dong, L. Sun. *ChemSusChem* **5**, 913 (2012).
23. L.-C. Song, M.-Y. Tang, F.-H. Su, Q.-M. Hu. *Angew. Chem., Int. Ed.* **45**, 1130 (2006).
24. L.-C. Song, M.-Y. Tang, S.-Z. Mei, J.-H. Huang, Q.-M. Hu. *Organometallics* **26**, 1575 (2007).
25. A. M. Kluwer, R. Kaprea, F. Hartl, M. Lutz, A. L. Spek, A. M. Brouwer, P. Van Leeuwen, J. N. H. Reek. *Proc. Natl. Acad. Sci. USA* **106**, 10460 (2009).
26. A. P. S. Samuel, D. T. Co, C. L. Stern, M. R. Wasielewski. *J. Am. Chem. Soc.* **132**, 8813 (2010).
27. P. Poddutoori, D. T. Co, A. P. S. Samuel, C. H. Kim, M. T. Vagnini, M. R. Wasielewski. *Energy Environ. Sci.* **4**, 2441 (2011).
28. X. Li, M. Wang, S. Zhang, J. Pan, Y. Na, J. Liu, B. Åkermark, L. Sun. *J. Phys. Chem. B* **112**, 8198 (2008).
29. S. A. Vinogradov, L.-W. Lo, D. F. Wilson. *Chem.—Eur. J.* **5**, 1338 (1999).
30. J. D. Lawrence, H. Li, T. B. Rauchfuss. *Chem. Commun.* **16**, 1482 (2001).
31. G. Si, W.-G. Wang, H.-Y. Wang, C.-H. Tung, L.-Z. Wu. *Inorg. Chem.* **47**, 8101 (2008).
32. W.-G. Wang, H.-Y. Wang, G. Si, C.-H. Tung, L.-Z. Wu. *Dalton Trans.* 2712 (2009).
33. J.-F. Capon, S. Ezzaher, F. Gloaguen, F. Y. Pétillon, P. Schollhammer, J. Talarmin. *Chem.—Eur. J.* **14**, 1954 (2008).
34. F. Wessendorf, J.-F. Gnichwitz, G. H. Sarova, K. Hager, U. Hartnagel, D. M. Guldi, A. Hirsch. *J. Am. Chem. Soc.* **129**, 16057 (2007).
35. C. Luo, D. M. Guldi, H. Imahori, K. Tamaki, Y. Sakata. *J. Am. Chem. Soc.* **122**, 6535 (2000).
36. R. F. Kelley, M. J. Tauber, M. R. Wasielewski. *J. Am. Chem. Soc.* **128**, 4779 (2006).
37. D. Rehm, A. Weller. *Isr. J. Chem.* **8**, 259 (1970).
38. J.-F. Côte, D. Brouillette, J. E. Desnoyers, J.-F. Rouleau, J.-M. St-Arnaud, G. Perron. *J. Solution Chem.* **25**, 1163 (1996).
39. H. Imahori, K. Tamaki, D. M. Guldi, C. Luo, M. Fujitsuka, O. Ito, Y. Sakata, S. Fukuzumi. *J. Am. Chem. Soc.* **123**, 2607 (2001).
40. H. Imahori, M. E. El-Khouly, M. Fujitsuka, O. Ito, Y. Sakata, S. Fukuzumi. *J. Phys. Chem. A* **105**, 325 (2001).

